

- ¹Y. Hazony, D. E. Earls, and I. Lefkowitz, Phys. Rev. **166**, N2, 507 (1968).
- ²T. J. Gleason and J. C. Walker, Phys. Rev. **188**, 893 (1969).
- ³M. J. Clauser, Phys. Rev. B **1**, 357 (1970).
- ⁴L. N. Matusevich and K. N. Schabalin, Zh. Prikl. Khim., **25**, 1157 (1952).
- ⁵V. A. Poperov and G. S. Zdanov, Z. Fiz. Khim. SSSR, **21**, 405 (1947); **21**, 521 (1947); **21**, 879 (1947); Structure Report XI, pp. 421-424 (unpublished).
- ⁶H. Toyoda, N. Niizeki, and S. Waku, J. Phys. Soc. Japan **15**, 10 (1960).
- ⁷A. Ya. Krasnikova, V. A. Koptsik, B. A. Strukov, and Wang Wing, Fiz. Tverd. Tela, **9**, 116 (1967) [Soviet Phys. Solid State **9**, 85 (1967)].
- ⁸S. Waku, H. Hirabayashi, H. Toyoda, H. Iwasaki, and R. Kiriya, J. Phys. Soc. Japan **14**, 973 (1959).
- ⁹S. Waku, K. Masuno, T. Tanaka, and H. Iwasaki, J. Phys. Soc. Japan **15**, 1185 (1960).
- ¹⁰G. E. Schacher, J. Chem. Phys. **46**, 3565 (1967).
- ¹¹A. Ya. Krasnikova and I. N. Polandov, Fiz. Tverd. Tela, **11**, 1753 (1969) [Soviet Phys. Solid State **11**, 1421 (1970)].
- ¹²R. Blinc, M. Brenman, and J. S. Waugh, J. Chem. Phys. **35**, (1961).
- ¹³D. E. O'Reilly and G. E. Schacher, J. Chem. Phys. **43**, 4222 (1965).
- ¹⁴R. Kiriya, H. Kiriya, T. Wada, N. Niizeki, and H. Hirabayashi, J. Phys. Soc. Japan **19**, 4 (1964).
- ¹⁵J. J. Rush, P. S. Leung, and T. I. Taylor, J. Chem. Phys. **45**, (1966).
- ¹⁶P. A. Montano, H. Shechter, A. Biran, and U. Shimony (unpublished).
- ¹⁷R. M. Housley, R. W. Grant and U. Gonser, Phys. Rev. **178**, 514 (1969).
- ¹⁸G. A. Bykov and Pham Zuy Xien, Joint Institute for Nuclear Research Report No. P-1231, 1962 (unpublished) [transl.: *Working Conference on the Mössbauer Effect, Proceedings of the Dubna Conference, 1962* (New York Consultants Bureau Enterprises, Inc. New York, 1963)].
- ¹⁹A. Ya. Krasnikova and V. A. Koptsik, Fiz. Tverd. Tela, **10**, 905 (1968) [Soviet Phys. Solid State **10**, 709 (1968)].
- ²⁰R. M. Housley and F. Hess, Phys. Rev. **146**, 517 (1966).
- ²¹W. Kerler, Z. Physik **167**, 194 (1962).
- ²²J. G. Dash, D. P. Johnson, and W. M. Visscher, Phys. Rev. **168**, 1087 (1968).
- ²³D. P. Johnson and J. G. Dash, Phys. Rev. **172**, 983 (1968).

Contribution of Some 4d and 5d Transition-Metal Ions on Octahedral Sites to the Anisotropy of Ferrites and Garnets*

P. Hansen

Philips Forschungslaboratorium Hamburg GmbH, 2000 Hamburg 54, Germany

(Received 8 September 1970)

The contribution to the magnetocrystalline anisotropy of transition-metal ions in ferrites on octahedral sites is calculated for the strong crystalline-field case for d^1 , d^2 , d^4 , and d^5 configurations. The single-ion model is used which requires small concentrations of such ions. Good agreement with experiment was found for trivalent ruthenium. For this case, anisotropy measurements of Ru^{3+} ($4d^5$)-doped yttrium-iron garnet of the composition $\text{Y}_{3-y}\text{Ca}_y\text{Fe}_{5-x}\text{Ru}_x\text{O}_{12}$ were carried out in the temperature range of 4.2-500°K. By fitting the theory to the measured anisotropy data, one finds for the product of the g factor times the exchange field, $gH_e = 1.1 \times 10^7$ Oe and the ratio of the trigonal field to the spin-orbit energy $v/\xi = -1$.

I. INTRODUCTION

The anisotropy of ferrites can be considerably influenced by very low concentrations of transition-metal ions¹⁻⁶ and rare-earth ions.^{7,8} In these cases, the spin-orbit coupling is an important parameter, since it measures the coupling energy of the spin in a certain direction. Thus, such ions contribute to the free energy due to the directional dependence of the magnetization. For the metal ions of the second- and third-transition series, the spin-orbit coupling is much higher than for the first transition-metal ions, so that especially for these elements a large contribution to the anisotropy may be expected.

Since only very little experimental or theoretical work is available in this field, the influence on the anisotropy will be calculated here for some of these ions with an md^n configuration for $n = 1, 2, 4, 5$.

The phenomenological energy expression for the magnetocrystalline anisotropy F is given in the case of cubic symmetry by

$$F = K_0 + K_1s + K_2p + K_3s^2 + \dots, \quad (1)$$

where

$$s = \alpha_1^2 \alpha_2^2 + \alpha_2^2 \alpha_3^2 + \alpha_1^2 \alpha_3^2, \quad p = \alpha_1^2 \alpha_2^2 \alpha_3^2.$$

The α_i are the direction cosines of the magnetization with respect to the cubic axes. The contribu-

tions ΔK_i of substituted ions to the crystal anisotropy constants K_i depend strongly on temperature. They are determined by the atomic structure of the material, and that mainly by the effective crystal-line fields, the spin-orbit coupling, and the exchange interaction. According to the order of magnitude of these interactions, the ΔK_i can be influenced considerably; e. g., the sign of K_i may change. This depends on the ions to be incorporated as well as on the ligands of the host lattice.^{9,10} The conditions for the 4d and 5d elements can be distinguished to a large extent from those of the 3d elements. For the latter, the energy splittings caused by the above-mentioned interactions may be arranged in decreasing order of magnitude according to the following series and garnets:

$$E_e > E_c \gg E_t > E_{\text{exch}} > E_{\text{SO}}. \quad (2a)$$

Quite a different series must be expected for 4d and 5d elements in ferrites:

$$E_c > E_e \gg E_{\text{SO}} \gtrsim E_t > E_{\text{exch}}. \quad (2b)$$

Here E_e denotes the energy of the electron interaction of the ions considered, E_c is the cubic crystal-field splitting, E_t represents the noncubic part of the crystal field locally produced by deformation. E_{SO} is due to the spin-orbit coupling, and finally E_{exch} is the splitting due to the exchange interaction with the magnetic neighbors. This important change in the relative magnitude of the energies as compared with the 3d elements, mainly arises from the strong decrease of the interelectronic repulsion¹¹ for these ions and the corresponding increase of the spin-orbit coupling.^{12,13} E_e and E_c are of the order of several 10^4 cm^{-1} , and all other interactions are smaller by at least a factor of 10. The relation $E_c > E_e$ implies especially that for the configurations d^4 to d^7 the ground state is the low-spin state.

Measurements of the saturation magnetization indicate that in the case of small concentrations the 4d and 5d ions occupy octahedral sites only, so that octahedral symmetry will be considered in the following. In that case E_t represents the splitting by a trigonal field.

The calculation of the anisotropy contributions ΔK_i as a function of these atomic parameters and the temperature leads to relatively simple formulas in the case of low-spin d^5 ions. In this case, only the exchange energy $g\mu_B H_e$ and the ratio of the trigonal field to the spin-orbit energy v/ξ (ξ is the one-electron spin-orbit coupling parameter, and v is the one-electron trigonal field parameter defined in Eq. (8) enter into the results as adjustable parameters, and for Ru^{3+} ($4d^5$), in particular, a comparison is possible with v/ξ -values of yttrium-gallium garnet (YGaG) from ESR measurements.¹⁴ Therefore, the influence of Ru^{3+} on the anisotropy constants of yttrium-iron garnet (YIG) has been studied for a

wide range of temperature.

With a suitable choice of $g\mu_B H_e$ and v/ξ a good fit of the theory to the experimental data up to room temperature is obtained.

II. THEORY

The single-ion model^{3,15} will be applied to the problem of calculating the contribution of such substituted ions to the anisotropy. The calculation of the dependence of the energy levels on the direction of magnetization, which accounts for the anisotropy, is based on the following assumptions:

(i) Only the splitting of the ground cubic term of the ion on an octahedral site by the spin-orbit coupling, the trigonal field, and the exchange interaction contributes to the anisotropy. The energy levels of this term are assumed to be the same for all octahedral sites except for the effects of exchange. Other interactions, such as the coupling with the lattice vibrations, are neglected.

(ii) The exchange interaction can be written within the molecular-field approximation in the form $\mathcal{H}_{\text{exch}} = g\mu_B \vec{H}_e \cdot \vec{S}$, where \vec{H}_e is the exchange field which is assumed to be paralleled to the direction of magnetization \vec{M} . \vec{S} is the spin of the substituted ion. The g factor is assumed to be isotropic which corresponds to an isotropic exchange interaction. Thus, possible deviations of the spins from the direction of \vec{H}_e for the adjacent ions are not taken into account. Furthermore, a temperature dependence of the exchange interactions is neglected.

The contribution of an ion to the free energy per unit volume is

$$F = -kT \sum_i N_i \ln z_i, \quad (3)$$

where

$$z_i = \sum_j e^{-E_{ij}/kT}. \quad (4)$$

i denotes the magnetically inequivalent sites and N_i the number of ions on these sites. The sum in (4) runs over all energy levels E_{ij} of the ion on site i . The anisotropy contributions ΔK_1 and ΔK_2 according to (1) are related to the free energy (3) in the three principal directions by

$$\Delta K_1 = 4[F(110) - F(100)], \quad (5)$$

$$\Delta K_2 = 9[3F(111) + F(100) - 4F(110)],$$

if the higher-order terms in Eq. (1) can be neglected.

A. d^1 and d^5 Ions

The transformation properties of the ground states of d^1 and d^5 configurations are identical in the strong-field limit. For both of them a sixfold degenerate ${}^2T_{2g}$ term is the lowest state on an octahedral site. The degeneracy is lifted by means of the Hamiltonian

$$\mathcal{H} = V_t(\vec{r}) + \lambda \vec{L} \cdot \vec{S} + g\mu_B \vec{S} \cdot H_{ex} S_x + \frac{1}{2} g\mu_B (H_{ex} S_x + H_{ey} S_y), \quad (6)$$

where

$$S_{\pm} = S_x \pm iS_y, \quad H_{ex} = H_{ex} \pm iH_{ey}.$$

$V_t(\vec{r})$ denotes the local trigonal field. The second term represents the spin-orbit coupling and can be written in this form as long as \mathcal{H} only operates within the manifold of states of the ${}^2T_{2g}$ ground state. λ is connected with the one-electron spin-orbit coupling parameter ξ by $\lambda = \xi$ for d^1 ions and by $\lambda = -\xi$ for low-spin d^5 ions, because for these ions in the octahedral field the t_{2g} orbitals always have the lowest energy due to the relation $E_c > E_e$. The t_{2g} orbitals are fully occupied with six electrons, so that the t_{2g}^5 configuration ($S = \frac{1}{2}$) can be regarded as a hole in the t_{2g} shell. A similar sign change occurs for the trigonal-field parameter in this case. The local trigonal axis, i. e., one of the (111) directions, was chosen as the quantization axis. In the simple case $H_e = 0$, the problem can easily be solved, and three magnetic doublets result with energies^{14,16}

$$E_g'' : E_0 = -\lambda \left[\frac{1}{2} + \frac{1}{3} (v/\lambda) \right], \quad (7)$$

$$E_g' : E_{\pm} = (\lambda/2) \left\{ \frac{1}{2} + \frac{1}{3} v/\lambda \pm \left[2 + \left(\frac{1}{2} - v/\lambda \right)^2 \right]^{1/2} \right\},$$

where the one-electron trigonal-field parameter v is conveniently defined as

$$\langle t_1^{\pm} | V_t(\vec{r}) | t_1^{\pm} \rangle = \langle t_2^{\pm} | V_t(\vec{r}) | t_2^{\pm} \rangle = -v/3, \quad (8)$$

$$\langle t_3^{\pm} | V_t(\vec{r}) | t_3^{\pm} \rangle = 2v/3.$$

E_g' and E_g'' designate the representations of the trigonal double group and indicate the transformation properties of the corresponding wave functions.

The t_i^{\pm} in Eq. (8) are linear combinations of the d functions, which are quantized along the trigonal axis and are of the form

$$\begin{aligned} t_1^{\pm} &= \left(\frac{2}{3}\right)^{1/2} \left| -2, \pm \frac{1}{2} \right\rangle + \left(\frac{1}{3}\right)^{1/2} \left| 1, \pm \frac{1}{2} \right\rangle, \\ t_2^{\pm} &= \left(\frac{2}{3}\right)^{1/2} \left| 2, \pm \frac{1}{2} \right\rangle - \left(\frac{1}{3}\right)^{1/2} \left| -1, \pm \frac{1}{2} \right\rangle, \\ t_3^{\pm} &= \left| 0, \pm \frac{1}{2} \right\rangle. \end{aligned} \quad (9)$$

The numbers in the ket $|m_L, m_S\rangle$ are the quantum numbers of the z component of the orbital and spin momentum. The functions (9) span a basis for the ${}^2T_{2g}$ state since they transform like the representation T_{2g} . The Hamiltonian (6) becomes diagonal for $H_e = 0$ for a special choice of linear combinations of (9) transforming like E_g' or E_g'' . From the transformation behavior of (9) with respect to the rotation of 120° around the z axis, it can easily be seen that both t_1^+ and t_2^+ transform in a unique way, whereas t_3^+ can couple together with t_1^+ , and t_3^+ can couple together with t_2^+ . Therefore, these wave functions are given by

$$\psi_1^0 = t_1^+, \quad \psi_2^0 = t_2^+,$$

$$\begin{aligned} \psi_1^+ &= at_3^+ + bt_1^+, & \psi_2^+ &= -at_3^+ + at_2^+, \\ \psi_1^- &= -bt_3^- + at_1^-, & \psi_2^- &= bt_3^- + at_2^-, \end{aligned} \quad (10)$$

where

$$a^2 + b^2 = 1, \quad a^2 = \frac{1}{2} \left(1 - \frac{\frac{1}{2} - v/\lambda}{\left[2 + \left(\frac{1}{2} - v/\lambda \right)^2 \right]^{1/2}} \right),$$

and the symbols 0, \pm correspond to those of the energies in (7).

The three magnetic doublets are now split by the exchange interaction. If the Hamiltonian operates upon the set of functions (10) a six-dimensional matrix is obtained which has to be diagonalized in the general case. The six levels are represented in Fig. 1 and are plotted vs v/ξ for $g\mu_B H_e/\xi = 0.5$ and $\vec{M} \parallel [001]$. The diagram corresponds to the d^5 configurations since $\lambda = -\xi$ then is negative. For d^1 ions, however, the order of levels has to be inverted. It appears that especially in this range even for still higher values of the exchange field the two lowest levels remain well separated from the higher levels. Therefore, the anisotropy of d^5 ions can be calculated in good approximation in terms of these lowest levels alone. This case will be investigated in some more detail.

Applying \mathcal{H} of Eq. (6) to the wave functions ψ_1^+ and ψ_2^+ , a quadratic secular equation is obtained. Its solutions are

$$E_j(\gamma_i) = E_{\pm} \pm \frac{1}{2} \Delta E(\gamma_i), \quad (11)$$

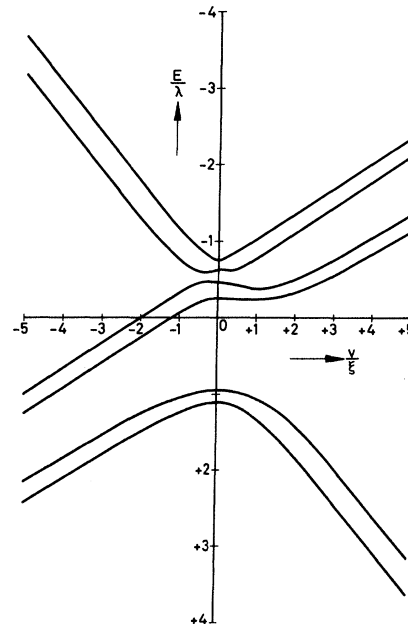


FIG. 1. Splitting of the ${}^2T_{2g}$ ground state of d^1 ($\lambda = +\xi$) and low-spin d^5 ($\lambda = -\xi$) ions on octahedral sites due to spin-orbit coupling, trigonal field and exchange field for $g\mu_B H_e/\xi = 0.5$ and $\vec{M} \parallel [001]$.

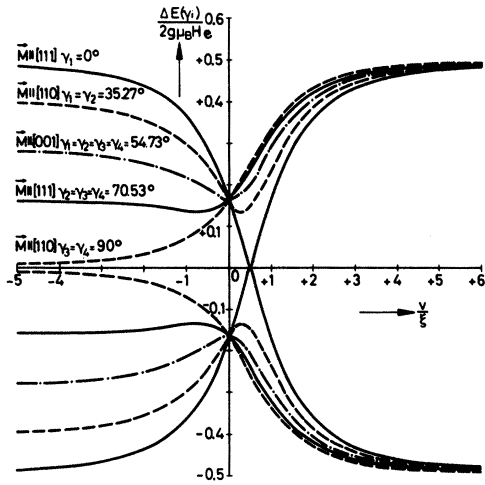


FIG. 2. Exchange splitting of the lowest magnetic doublet of low-spin d^6 ions.

$$\Delta E(\gamma_i) = g\mu_B H_e [(1 - 2a^2)^2 \cos^2 \gamma_i + a^4 \sin^2 \gamma_i]^{1/2},$$

where γ_i is the angle between \vec{M} and one of the four possible [111] directions. Thus, the splitting depends only on the parameters H_e and v/ξ .

According to the resonance measurements it is useful to assume that the magnetization lies in a (110) plane. Then the γ_i may be expressed by the angle θ between \vec{M} and the [001] direction in this plane by

$$\begin{aligned} \cos \gamma_1 &= (\frac{1}{3})^{1/2} \cos \theta + (\frac{2}{3})^{1/2} \sin \theta, \\ \cos \gamma_2 &= (\frac{1}{3})^{1/2} \cos \theta - (\frac{2}{3})^{1/2} \sin \theta, \\ \cos \gamma_3 &= \cos \gamma_4 = (\frac{1}{3})^{1/2} \cos \theta. \end{aligned} \quad (12)$$

γ_1 and γ_2 are the angles between \vec{M} and the [111] directions in the (110) plane of \vec{M} , and γ_3 and γ_4 are those of the other (110) plane, and therefore always include the same angle with \vec{M} .

The magnitude of $\Delta E(\gamma_i)$ is strongly influenced by the sign and the absolute value of v/ξ . This is shown in Fig. 2 for some directions of magnetization, which occur in Eq. (5), and for different sites i . As expected, the dependence on the direction of

magnetization becomes very small for large positive v/ξ , since then an orbital singlet is the lowest level. However, in all other cases, except for $v/\xi = 0$, a strong direction-dependent splitting is caused by H_e , so that a large anisotropy contribution can be predicted.

From Eqs. (3)–(5), (11), and (12) ΔK_1 and ΔK_2 can be calculated as a function of v/ξ , H_e , and T , but the resulting formulas become very complicated and, therefore, it appears more convenient to study the two special cases $\Delta E(\gamma_i) \gg kT$ and $\Delta E(\gamma_i) \ll kT$. In order to calculate the exact temperature dependence of ΔK_i , the computer was used.

In the first case, Eq. (3) reduces to the simple form

$$F = - (N/8) [\Delta E(\gamma_1) + \Delta E(\gamma_2) + 2 \Delta E(\gamma_3)], \quad (13)$$

where a statistical distribution has been assumed so that $N_i = \frac{1}{4}N$. If then the γ_i in (13) is expressed explicitly by θ according to Eq. (12), the free energy (13) can be expanded in powers of s and p according to Eq. (1) in the range $v/\xi \gtrsim -\frac{1}{2}$. For ΔK_1 and ΔK_2 the following relations are obtained:

$$\Delta E(\gamma_i) \gg kT \begin{cases} \Delta K_1 = \frac{Ng\mu_B H_e}{4\sqrt{3}} [(1 - 2a^2)^2 + 2a^4]^{1/2} \epsilon^2 \\ \Delta K_2 = -\frac{Ng\mu_B H_e}{4\sqrt{3}} [(1 - 2a^2)^2 + 2a^4]^{1/2} \\ \quad \times (6 - 5\epsilon)^3, \end{cases} \quad (14)$$

where

$$\epsilon = \frac{a^4 - (1 - 2a^2)^2}{2a^4 + (1 - 2a^2)^2}. \quad (15)$$

Thus, ΔK_1 is always positive. ΔK_2 , however, is positive for $v/\xi > 0$ and negative for $v/\xi < 0$. In the range $v/\xi \lesssim -\frac{1}{2}$, ϵ is close to 1, and the convergence is not sufficient. Then the free energy according to Eq. (13) has to be used. But generally the ratio $\Delta K_2/\Delta K_1$ only depends on v/ξ at low temperatures. Therefore, it can be assumed that the fit of $\Delta K_2/\Delta K_1$ to the observed anisotropy data at 4.2°K will give at least an estimate of the quantity v/ξ .

For high temperatures, Eq. (3) can always be written accurately in the form of Eq. (1), yielding the anisotropy contributions

$$\Delta E(\gamma_i) \ll kT \begin{cases} \Delta K_2 = -\frac{16}{15} kTN [(1 - 2a^2)^2 - a^4]^3 \left(\frac{g\mu_B H_e}{2\sqrt{3}kT} \right)^3 \left[1 - \frac{17}{14} \left(\frac{g\mu_B H_e}{2ckT} \right)^2 + \dots \right] \\ \Delta K_1 = \frac{1}{3} kTN [(1 - 2a^2)^2 - a^4]^2 \left(\frac{g\mu_B H_e}{2\sqrt{3}kT} \right)^4 \left[1 - \frac{4}{5} \left(\frac{g\mu_B H_e}{ckT} \right)^2 + \frac{17}{70} \left(\frac{g\mu_B H_e}{ckT} \right)^4 - \dots \right], \end{cases} \quad (16)$$

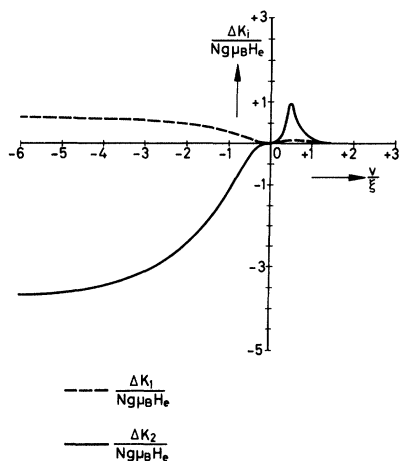


FIG. 3. Contribution of low-spin d^5 ions to the anisotropy at 0°K.

where

$$c = \sqrt{3} / [(1 - 2a^2)^2 + 2a^4]^{1/2}.$$

Thus, especially the ratio $\Delta K_2 / \Delta K_1$ is proportional to $(\mu_B H_e / kT)^2$ and this means that ΔK_2 is a sensitive measure for the exchange field at high temperatures. But as the explicit results obtained in (14) and (16) are only correct to the first-order perturbation theory in the energy levels, higher-order terms in the expansion require an extension to the next higher

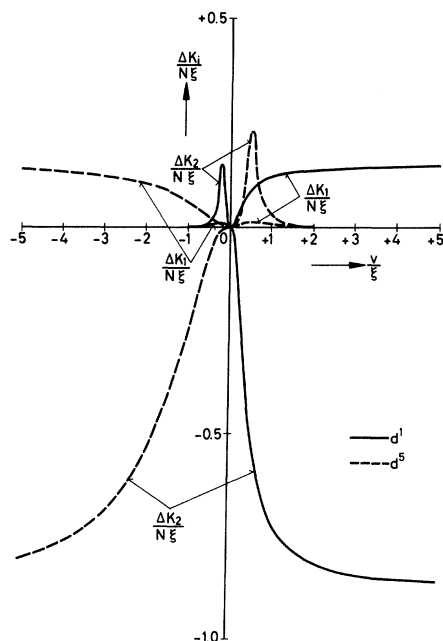


FIG. 4. Contribution of d^1 and low-spin d^5 ions to the anisotropy at 0°K.

approximation. Then matrix elements to the higher magnetic doublet must be taken into account. This leads to very complicated relations and will not be considered further. ΔK_3 remains small and attains at least the order of ΔK_1 at very low temperatures.

Analogous results may be derived for d^1 ions for $v/\xi \lesssim -1$. Then, however, a^2 has to be replaced by $1 - a^2$.

In all other cases the relations for the ΔK_i become rather complicated. Therefore, some results are represented in the following figures. Figure 3 shows a plot of ΔK_1 and ΔK_2 for d^5 ions, using Eqs. (5), (11), and (13). A sign change occurs for ΔK_2 at $v/\xi = 0$. Especially for YIG with a negative trigonal field¹⁴ a negative value of ΔK_2 is expected.

In Fig. 4 the general case is represented according to the energy-level diagram of Fig. 1 for $g\mu_B H_e / \xi = 0.5$ for d^1 and d^5 ions. Finally, Fig. 5 represents the influence of the exchange field for d^5 ions. Up to values $g\mu_B H_e / \xi \lesssim 0.6$ the ΔK_i are proportional to H_e . For higher exchange fields, the deviation from linearity increases due to the coupling to the higher levels E_0 and E_- .

B. d^2 and d^4 Ions

The octahedral ground term of d^2 and d^4 ions is a ${}^3T_{1g}$ state in the strong-field limit because the d^4 configuration t_{2g}^4 again may be viewed as a state with two holes in the t_{2g} shell and thus corresponds to d^2 with respect to the transformation properties. To proceed further, a suitable set of wave functions

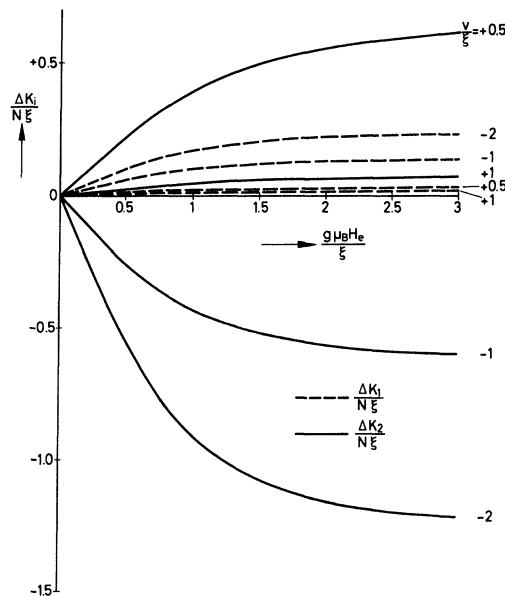


FIG. 5. Influence of increasing exchange field to the anisotropy of low-spin d^5 ions at 0°K.

must be given which transform like T_{1g} . Applying the usual spinfunctions α and β , three symmetrical functions can be constructed with a total spin $S = 1$:

$$\begin{aligned}\varphi_1 &= \alpha(1)\alpha(2), \\ \varphi_0 &= (1/\sqrt{2}) [\alpha(1)\beta(2) + \alpha(2)\beta(1)], \\ \varphi_{-1} &= \beta(1)\beta(2),\end{aligned}\quad (17)$$

where the numbers in parentheses designate the two electrons or holes.

The subscripts are the quantum numbers m_s of the z component of the total spin, and the axis of quantization is again the trigonal axis. The corresponding orbital functions have to be antisymmetrical.

Using the orbital part t_i of (9), the following functions are obtained:

$$\begin{aligned}\psi_1 &= (1/\sqrt{2}) [t_1(1)t_3(2) - t_3(1)t_1(2)], \\ \psi_2 &= (1/\sqrt{2}) [t_2(1)t_3(2) - t_3(1)t_2(2)], \\ \psi_3 &= (1/\sqrt{2}) [t_1(1)t_2(2) - t_2(1)t_1(2)],\end{aligned}\quad (18)$$

with the desired transformation properties which can easily be verified by means of the corresponding characters. Moreover, they are diagonal with respect to rotation by 120° around the trigonal axis, since the original functions t_i have this property. Combining (17) and (18), the nine functions

$$t_i^{m_s} = \psi_i \cdot \varphi_{m_s}, \quad i = 1, 2, 3, \quad m_s = 0, \pm 1 \quad (19)$$

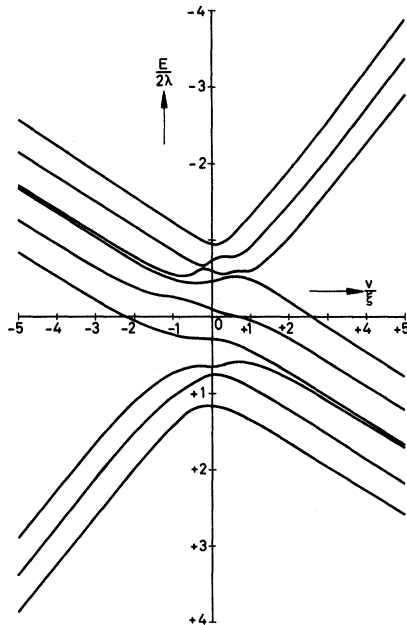


FIG. 6. Splitting of the ${}^3T_{1g}$ ground state of d^2 ($\lambda = +\frac{1}{2}\xi$) and low-spin d^4 ($\lambda = -\frac{1}{2}\xi$) ions on octahedral sites due to spin-orbit coupling, trigonal field and exchange field for $g\mu_B H_e/\xi = 0.5$ and $\bar{M} \parallel [001]$.

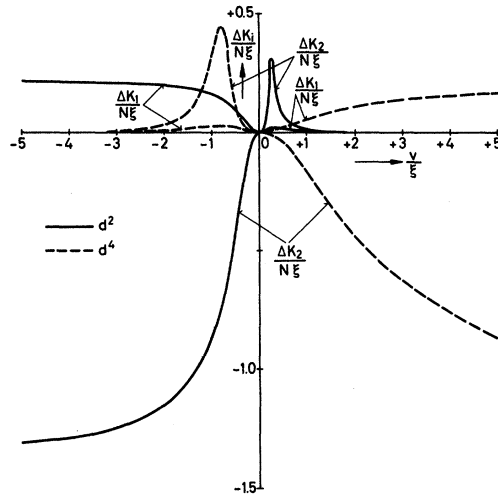


FIG. 7. Contribution of d^2 and low-spin d^4 ions to the anisotropy at 0°K .

can be constructed which span a basis to ${}^3T_{1g}$. In the simple case $H_e = 0$, it follows from the representations of the trigonal double group that the ninefold degeneracy is partly removed and 3 doublets and 3 singlets result according to

$${}^3T_{1g} \rightarrow 3E_g + 2A_{1g} + A_{2g}.$$

Thus, the secular equation reduces to a simple form and can explicitly be expressed in terms of v and ξ .¹⁶ For $H_e \neq 0$ the Hamiltonian (6) has to be applied to the set of wave functions (19), and then the problem becomes much more complicated, except for $g\mu_B H_e/\xi \ll 1$.¹⁷ However, this condition does not hold generally and thus no explicit formulas will be derived. Therefore, the computed solutions of the nine-dimensional problem are represented in Fig. 6 for $g\mu_B H_e/\xi = 0.5$ and $\bar{M} \parallel [001]$. For d^2 we have $\lambda = \frac{1}{2}\xi$, and for d^4 , $\lambda = -\frac{1}{2}\xi$, so that the energy-level diagram in Fig. 6 corresponds to d^4 and must be inverted for d^2 .

In the limit $T = 0^\circ\text{K}$, again only the lowest energy level is occupied. From Eqs. (5), (12), and (13) the contributions to the anisotropy can be calculated. The result is given in Fig. 7 for d^2 and d^4 ions with $g\mu_B H_e/\xi = 0.5$. As expected from the energy-level diagram, d^2 ions are highly anisotropic for negative values of v/ξ since then an orbital doublet is the lowest and d^4 ions are highly anisotropic for positive values of v/ξ . In this case two singlets are the lowest levels lying very close together so that they behave like an orbital doublet.

A comparison of the different configurations shows that ΔK_1 is positive in all cases while the sign of ΔK_2 is determined by v/ξ . The magnitude of the anisotropy contributions for positive v/ξ is roughly of the same order for d^2 and d^4 and in a

small range $0 \lesssim v/\xi \lesssim 1$ for d^4 and d^5 . For negative v/ξ , d^2 and d^5 show a similar behavior. In the various cases the absolute magnitude and the sign of ΔK_2 , however, strongly depend on the particular values of the respective parameters H_e , ξ , and v/ξ . The same is true for the temperature dependence which is, therefore, discussed only in connection with the experimental results.

III. EXPERIMENTS

As pointed out above, it appears to be most suitable for a comparison with the theory to study the anisotropy contribution of a low-spin d^5 ion such as Ru^{3+} in YIG. In this case, only the two parameters v/ξ and H_e enter into the theoretical expressions for ΔK_1 and ΔK_2 , and thus they may be determined from a fit to the experimental data. This is correct, if the condition $g\mu_B H_e/\xi \lesssim 0.6$ is satisfied, which can be assumed to be valid for this case, and thus only the lowest energy levels contribute to the anisotropy.

Therefore, materials of the compositions $\text{Y}_{3-y}\text{Ca}_y\text{Fe}_{5-x}\text{Ru}_x\text{O}_{12}$ were investigated.^{17,18} The single crystals were grown from $\text{PbO}/\text{PbF}_2/\text{B}_2\text{O}_3$ flux at about 1100 °C.¹⁹ Very pure materials were used, i. e., especially the content of rare-earth impurities was of the order of 1 ppm. The content of Ca and Ru is given in Table I. The crystals containing calcium were grown to investigate whether Ca may introduce Ru^{4+} ions.

Measurements were performed on spheres of 0.07-cm diameter applying the method of ferromagnetic resonance at 9.25 GHz in the temperature range of 4.2–500 °K. By neglecting the higher-order terms in (1), K_1/M_s and K_2/M_s were obtained from the resonant field in the three principal directions using the relations

$$\begin{aligned} \omega/\gamma &= H_R(001) + 2K_1/M_s, \\ \omega/\gamma &= H_R(111) - \frac{4}{3}K_1/M_s - \frac{4}{9}K_2/M_s, \\ \omega/\gamma &= [H_R(110) - 2K_1/M_s]^{1/2} \\ &\quad \times [H_R(110) + K_1/M_s + \frac{1}{2}K_2/M_s]^{1/2} \end{aligned}$$

where $H_R(klm)$ is the resonant field in the $[klm]$ direction in a (110) plane.

Since $x \ll 1$, the influence of x on the saturation magnetization could be neglected, and thus $K_1(T)$ and $K_2(T)$ could be calculated from the measured values of K_1/M_s and K_2/M_s using $M_s(T)$ of the un-

TABLE I. Composition of the measured single crystals.

Material	Composition	$x \pm 0.01$	$y \pm 0.005$
(a)		< 0.01	0
(b)	$\text{Y}_{3-y}\text{Ca}_y\text{Fe}_{5-x}\text{Ru}_x\text{O}_{12}$	0.02	0
(c)		0.01	0.01

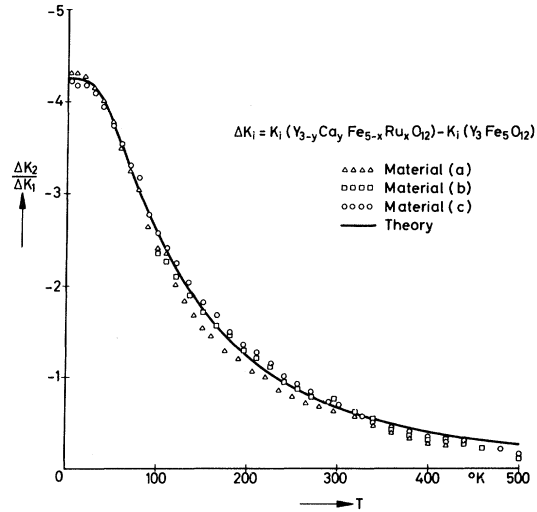


FIG. 8. Temperature dependence of the ratio $\Delta K_2/\Delta K_1$ of the anisotropy contributions due to Ru^{3+} in YIG. The theoretical curve is based on the values $v/\xi = -1.0$ and $gH_e = 1.1 \times 10^7$ Oe.

doped YIG. Thus the anisotropy contributions ΔK_1 and ΔK_2 due to the ruthenium are given by

$$\Delta K_i = K_i(x) - K_i(0). \quad (20)$$

For the material (c) (see Table I) an additional difficulty arises from the calcium content. It might be possible that both Ru^{4+} and Fe^{4+} are present besides Ru^{3+} . The anisotropy contribution of Fe^{4+} , however, can be neglected, but that of Ru^{3+} and Ru^{4+} may be of the same order in the range of expected v/ξ values. However, if the parameter values of v/ξ and H_e are assumed to be approximately the same, the temperature dependence of ΔK_i of these ions is different. In particular, in the case of a considerable concentration of Ru^{4+} , the temperature behavior of the ratio $\Delta K_2/\Delta K_1$ must be different from that of the materials (a) and (b), which contain only Ru^{3+} . In Fig. 8 the measured values of $\Delta K_2/\Delta K_1$ according to Eq. (20) are represented for the three materials. Apart from small deviations, they show the same temperature behavior. Therefore, a composition $\text{Y}_{3-y}\text{Ca}_y\text{Fe}_{5-x}\text{Ru}_x^{3+}\text{Fe}_y^{4+}\text{O}_{12}$ of the material (c) seems to be present, and a negligible Ru^{4+} concentration can be assumed. A similar result is obtained from anisotropy measurements of iridium-doped YIG of the composition $\text{Y}_{3-y}\text{Ca}_y\text{Fe}_{5-x}\text{Ir}_x\text{O}_{12}$.¹⁷ They show that only very low Ir^{4+} ($5d^5$) concentrations are present. This can be deduced from the fact that Ir^{3+} ($5d^6$) is nonmagnetic in the low-spin state ($S=0$) and thus does not contribute to the anisotropy which, therefore, can be influenced only by Ir^{4+} . Consequently, it is reasonable to assume the ruthenium

ion to be also preferably in the trivalent state. In a recently published paper,²⁰ anisotropy measurements of $Y_3Fe_{5-2x}Ru_xZn_xO_{12}$ have been reported showing also negative values of $\Delta K_2/\Delta K_1$. But the results are discussed in terms of Ru^{4+} which does not seem to be justified as this ion gives a positive ΔK_2 in the range of $v/\xi < 0$.

Moreover, Fig. 8 shows that $\Delta K_2/\Delta K_1$ is independent of the concentration, as expected. It is negative, and so v/ξ also has to be negative. As mentioned in Sec. II the ratio $\Delta K_2/\Delta K_1$ depends only on v/ξ at low temperatures. Therefore, the theoretical curve, which was calculated from Eqs. (3)–(5), (11), and (12), was fitted to the average value of $\Delta K_2/\Delta K_1$ of the materials (a) and (c) at 4.2 °K yielding $v/\xi = -1$. The uncertainty in the fit leads to an error in v/ξ of ± 0.05 with respect to these two materials and might be slightly higher if some more materials were investigated. The crystal (b) could only be measured down to 100 °K. For lower temperatures, the anisotropy and the linewidth become very large and no accurate measurements of the resonant fields could be made. In order to determine the exchange field, the whole temperature behavior below 295 °K was fitted again to the average values, yielding the result $gH_e = 1.1 \times 10^7$ Oe. With these values the energy-level diagram of Ru^{3+} in YIG was drawn according to Fig. 9. The free-ion value ξ of Ru^{3+} is about 1500 cm^{-1} .¹⁰ If the amount of reduction is assumed to be 25%, then the separation of the energy levels E_+ and E_0 corresponds to 1400 cm^{-1} for $v/\xi = -1$. The exchange splitting becomes a maximum if \vec{M} lies parallel to a [111] direction ($\gamma_1=0$), as is shown in Fig. 2. At higher temperatures the agreement of theory and experiment is not as good due to the assumption of a temperature-independent exchange field.

In addition, the concentration can be determined by fitting the theory to the absolute value of ΔK_2 at $T=4.2 \text{ °K}$, and the values obtained are not at variance with the chemical analysis. The latter is, however, not very accurate. In Table II the results

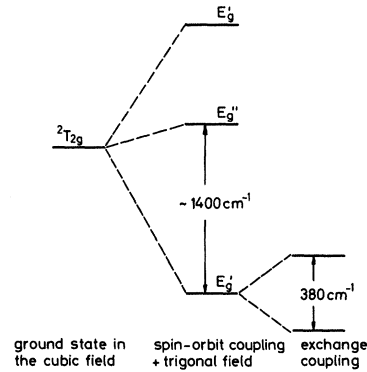


FIG. 9. Splitting of the ${}^2T_{2g}$ ground state of Ru^{3+} ($4d^5$) in YIG ($v/\xi = -1$). The primed representations are of the double trigonal group. The exchange splitting corresponds to $M \parallel [111]$.

obtained for Ru^{3+} are summarized. The comparison with Co^{2+} points out the strong effect of Ru^{3+} .

Furthermore, these results can be compared with electron-spin-resonance measurements of ruthenium-doped YIG from which v/ξ is found to be -1.06 ,¹⁴ which agrees very well with our data. A qualitative agreement was expected since the difference of the ionic radii of Ga^{3+} and Fe^{3+} is small. Thus, it is reasonable to assume that the crystal-field parameters, and so the value of v/ξ , are very close to those of YIG.

IV. CONCLUSIONS

In the strong-crystal-field limit, the energy splitting of the ground state was determined for the d^1 , d^2 , d^4 , and d^5 configurations, from which the anisotropy contributions were calculated. ΔK_1 turns out to be positive for all configurations in the whole range of v/ξ values. ΔK_2 , however, changes the sign with v/ξ .

For $Ru^{3+}(4d^5)$ -doped YIG, it could be shown that the anisotropy values measured can be described successfully within the scope of the single-ion mod-

TABLE II. Contributions of Ru^{3+} to the anisotropy of YIG.

Material	T (°K)	K_1 _{expt} $\times 10^4$ (erg/cm ³)	K_2 _{expt} $\times 10^4$ (erg/cm ³)	$\Delta K_1/N$ (cm ⁻¹)	$\Delta K_2/N$ (cm ⁻¹)	gH_e $\times 10^7$ (Oe)	v/ξ
(a)		1.97	-19.8				
(b)	4.2	70	-300		
(c)		19.4	-93.3				
(a)		0.04	-3.9				
(b)	130	15.2	-40.3	28	-60	1.1	-1.0
(c)		7.9	-21.2				
(a)		0.26	-0.23				
(b)	295	1.9	-2.0	5	-4		
(c)		0.8	-1.1				
Co-YIG (Ref. 3)	4.2	11	-46	29	-100	0.4	...

el and with an isotropic exchange interaction. The contribution to the anisotropy per ion of Ru^{3+} in YIG is very large, about 2 to 3 times larger than that of Co^{2+} . The value of v/ξ is negative in agreement with ESR measurements on YGaG and amounts to -1 . The exchange interaction between Ru^{3+} and Fe^{3+} is found to be substantially larger than that between the iron ions. It should be noted that the error due to the relatively large uncertainty in the concentration of Ru^{3+} ions does not affect the obtained values of v/ξ and gH_e because they are deduced from the ratio $\Delta K_2/\Delta K_1$. It may be mentioned that these results do not only apply for the ruthenium-doped YIG, but in the main also for ruthenium-doped lithium ferrite.²¹ Here, ΔK_1 also is positive and ΔK_2 negative, and thus the value of

v/ξ is negative.

Above room temperature, the agreement of theory and experiment is not as good, but in this range it is no longer justified to neglect the temperature dependence of the exchange field.

By additionally incorporating Ca, Mg,¹⁷ or Zn,²⁰ it could be found that the concentration of Ru^{4+} ions is negligible and, therefore, Fe^{4+} ions are probably present.^{22,23}

ACKNOWLEDGMENTS

The author would like to express his thanks to Dr. W. Tolksdorf who grew and prepared the single-crystal specimens, Dr. J. Verweel for helpful discussions, and P. Bressler and J. Schuld for technical assistance.

*An essential part of this article is contained in a thesis (Ref. 17).

¹L. R. Bickford, J. M. Brownlow, and R. F. Penoyer, Proc. IEEE Suppl. 5 104B, 238 (1957).

²G. Elbinger, Phys. Status Solidi 9, 843 (1965).

³M. D. Sturge, E. M. Georgy, R. C. LeCraw, and J. P. Remeika, Phys. Rev. 180, 413 (1969).

⁴A. Broese van Groenou, P. F. Bongers, and A. L. Stuyts, Mater. Sci. Eng. 3, 317 (1969).

⁵P. K. Baltzer, J. Phys. Soc. Japan Suppl. 17, 192 (1961).

⁶A. J. Pointon and J. M. Robertson, Phil. Mag. 17, 703 (1968).

⁷R. F. Pearson and R. W. Cooper, J. Phys. Soc. Japan Suppl. 17, 396 (1961).

⁸R. F. Pearson, J. Appl. Phys. 33, 1236 (1962).

⁹C. K. Jørgenson, *Absorption Spectra and Chemical Bonding in Complexes* (Pergamon, Oxford, England, 1962).

¹⁰H. L. Schläfer and G. Gliemann, *Einführung in die Ligandenfeldtheorie* (Akademische Verlags Gesellschaft, Frankfurt am Main, 1967).

¹¹L. E. Orgel, *An Introduction to Transition Metal*

Chemistry: Ligand Field Theory (Wiley, New York, 1960).

¹²P. B. Dorain and R. G. Wheeler, J. Chem. Phys. 45, 1172 (1966).

¹³P. B. Dorain, H. H. Patterson, and P. C. Jordan, J. Chem. Phys. 49, 3845 (1968).

¹⁴I. A. Miller and E. L. Offenbacher, Phys. Rev. 166, 269 (1967).

¹⁵J. C. Slonczeski, Phys. Rev. 110, 1341 (1958).

¹⁶K. W. H. Stevens, Proc. Roy. Soc. (London) A219, 542 (1953).

¹⁷P. Hansen, Philips Res. Rept. Suppl. No. 7 (1970).

¹⁸P. Hansen and W. Tolksdorf, J. Phys. (Paris) (to be published).

¹⁹W. Tolksdorf, J. Cryst. Growth 3, 463 (1968).

²⁰R. Krishnan, Phys. Status Solidi 1, K17 (1970).

²¹P. Hansen (unpublished).

²²J. Verweel and B. M. Roovers, *Solid State Physics in Electronics & Telecommunications* (Academic, London, 1960), Vol. 3, p. 475.

²³K. Nassau, J. Cryst. Growth 2, 215 (1968).

Influence of Spin-Orbit Scattering on the s - d Exchange Model

B. Giovannini*

Department of Physics, University of California, Los Angeles, California 90024

(Received 20 April 1970)

Starting with an Anderson Hamiltonian for a metallic system with impurities, adding to it a spin-orbit scattering term for the conduction electrons, and performing a Schrieffer-Wolff canonical transformation, one induces an s - d model which takes into account spin-orbit scattering in a consistent fashion. The Hamiltonian derived in this way is used to discuss the alteration of the Kondo effect to lowest order in perturbation theory (for $T \gg T_K$) and the EPR residual linewidth.

I. INTRODUCTION

Since Kondo's¹ discovery of a logarithmic divergence in perturbation theory for the scattering of

conduction electrons from magnetic impurities in metals, a large amount of experimental and theoretical work has been devoted to this problem.² Recently, Heeger² suggested that the Kondo effect